Identification of the barstar binding site of barnase by NMR spectroscopy and hydrogen–deuterium exchange

David N.M. Jones, Mark Bycroft, Michael J. Lubienski, Alan R. Fersht*

MRC Unit for Protein Function and Design, Cambridge Centre for Protein Engineering, Department of Chemistry, University of Cambridge, Lensfield Road, Cambridge CB2 1EW, UK

The extracellular ribonuclease from *Bacillus amyloliquifaciens*, barnase, forms a tightly-bound one-to-one complex with its intracellular inhibitor barstar. The barstar binding site on barnase was characterised by comparing the differences in the chemical shift and hydrogen–deuterium exchange rates between free and bound barnase Chemical shift assignments of barnase in the complex with barstar were determined from 3D NOESY-HMQC and TOCSY-HMQC spectra of a complex that had been prepared with uniformly ^{15}N-labelled barnase and unlabelled barstar. Hydrogen exchange rates were obtained from an analysis of a series of [^{15}N]HMQC spectra of a sample prepared in the same manner exchanged into D_2O. The largest changes in either chemical shift or hydrogen–deuterium exchange rate are observed for residues located in the active-site and substrate binding loops indicating that barstar inhibits barnase activity by sterically blocking the active site.

Barnase–barstar complex; NMR assigment

1. INTRODUCTION

The formation of specific protein–protein complexes is of fundamental importance in many biological processes. Consequently, an understanding of the nature and magnitude of the forces involved in protein–protein recognition is of considerable interest [1]. The extracellular ribonuclease, barnase, from *Bacillus amyloliquefaciens* forms a tightly bound 1:1 complex with its natural polypeptide inhibitor, barstar. This complex forms rapidly on mixing of the two components and is stable for long periods of time. These properties make it a suitable system for the study of the nature of the forces at the interface of protein–protein complexes.

Barnase is a guanine-preferential endo-ribonuclease and is related by its similarities in sequence and fold to a series of other fungal and bacterial ribonucleases [2]. It consists of a single polypeptide chain of 110 amino acids ($M_r = 12,382$) which forms two N-terminal α-helices and a five-stranded anti-parallel β-sheet. The main hydrophobic core is formed by the packing of the first α-helix against the β-sheet. On the other side of the β-sheet a broad shallow groove runs almost the entire length of the molecule. Residues, His-102, Glu-73 and Arg-87, which are strictly conserved within the family of ribonucleases, are located in the shallow groove and form the active site. A conserved loop formed by residues 56–69 [2,3] lies at one end of the broad groove and is involved in binding the guanine base of the substrate. The three-dimensional structure of barnase has been well characterised by X-ray crystallography [4,5] and the solution structure has been determined by ^{1}H-NMR spectroscopy in this laboratory [6,7].

In contrast, relatively little is known about the structure or properties of barstar. It consists of a single polypeptide chain of 89 amino acids ($M_r = 10,200$) and is produced by *Bacillus amyloliquefaciens* as a specific intracellular inhibitor of barnase [8]. It has been shown that the simultaneous expression of barstar is an absolute requirement for the expression of active barnase in *E. coli* [9]. Barstar interacts with barnase to form a tightly bound one-to-one complex [10] with an association rate constant of 5×10^8 M^{-1} s^{-1} and a dissociation rate constant of 10^{-5} s^{-1} [11].

In this paper, the location of the barstar binding site on barnase was investigated by comparing changes in amide–proton chemical shifts and hydrogen–deuterium exchange rates when barstar binds to ^{15}N-labelled barnase. Our results suggest that barstar interacts primarily with the active site and the guanosine-binding loops of barnase but, in addition, the binding site extends almost the whole length of the molecule and may involve other regions which are putative subsites involved in RNA hydrolysis [12].

*Corresponding author.

2. MATERIALS AND METHODS

2.1. Materials

SP-Trisacryl was purchased from IBF and dialysis tubing with M_r cut-off 3500 was obtained from Spectrum Medical Industries. Ultrafiltration cells and membranes were purchased from Amicon [^{15}N]Ammonium chloride (98 atom%) was purchased from Aldrich.

2.2. Protein expression and purification

Wild-type barnase was purified from cultures of *Escherichia coli* containing the plasmid pMT410 [13] as described previously [14] except that the casein amino acid hydrolysate was omitted from the medium and the ammonium chloride was replaced with [^{15}N]ammonium chloride (98 atom%).

The barstar plasmid was constructed by cloning the *EcoRI-Hind*III fragment of pMT410, which contains the barnase and barstar genes, into the polylinker region of pTZ18U (Pharmacia). Dideoxy sequencing revealed a discrepancy between the published sequence starting at nucleotide 624, located at the end of the barnase gene: CCGGCCTCT-A [13]; and the sequence of our DNA: CCGAGCTCTA. The latter sequence contains a *Sac*I site (GAGCTC) which allowed the removal of the barnase alkaline-phosphotase promoter sequence and the barnase gene by *Sac*I digestion to give the barstar plasmid pML2bs. This was transformed into *E coli* strain BL21(DE3)[pLysE] [15].

Barstar was purified from cultures grown in 2×TY medium containing ampicillin and chloramphenicol. Barstar expression was induced by the addition of IPTG (to a final concentration of 0.5 mM) at an $OD_{600} = 2 0$. The cultures were harvested when they reached stationary phase. The cells were lysed by ultrasonication and the resulting supernatent cut twice with ammonium sulphate. Barstar was found to precipitate in the 40–80% cut. This fraction was purified by gel filtration on a Sephadex G75 Superfine (Pharmacia) column followed by FPLC on a Mono-Q 10/10 column. The resulting protein appeared as a single band when analysed by SDS-PAGE and IEF gel electrophoresis (pI 4.55). The protein was flash-frozen in liquid N_2 and stored frozen at −70°C.

2.3 Sample preparation

Samples of barnase were prepared from lyophilised protein stored at −20°C. Samples of barstar were prepared from frozen stock solutions: the samples were thawed and concentrated in an Amicon 8MC Ultrafiltration cell to a final concentration of 3–4 mM in 10 mM d$_{11}$-Tris/HCl buffer adjusted to pH 6.6. For exchange studies, samples were exchanged into D_2O buffer containing 10 mM d$_{11}$-Tris/HCl and the pH adjusted to 6 15 with DCl/NaOD (uncorrected for isotope effect)

2.4. NMR spectroscopy

All NMR experiments were carried out on a Bruker AMX 500 spectrometer. Chemical shifts for protons are given relative to external TSP (0.0 ppm) and ^{15}N chemical shifts quoted relative to external ammonium chloride (2.9 M in 1M HCl) set at 24.93 ppm [16].

2D ^{1}H–^{15}N HSQC spectra were acquired using the pulse sequence described by Bax et al. [17] and 2D HMQC-NOESY spectra were obtained using the pulse sequence reported by Gronenborn et al. [18]. 3D NOESY-HMQC and TOCSY-HMQC were recorded essentially as described by Marion et al. [19]. 2D ^{15}N-edited NOESY were acquired by using the same pulse sequence as the 3D NOESY-HMQC experiment except that the normally incremented delay in the ^{15}N dimension was fixed at 3 μs.

3. RESULTS

3.1. Amide chemical-shift assignments of free barnase

The ^{15}N assignments of free barnase (Fig. 1A) were made by comparison of the ^{1}H–^{15}N HSQC spectrum with the previous ^{1}H chemical shift assignments [6] and from the *J* coupling correlations established from a 3D TOCSY-HMQC spectrum [19] Any ambiguities were resolved by inspection of the 3D NOESY-HMQC spectrum. The assignments of the amide ^{1}H and ^{15}N chemical shifts in free barnase are listed in Table I.

3.2. Assignments of barnase in the complex with barstar

Initial assignments in the spectrum of the complex were made by a direct comparison with the spectrum of the free enzyme. These assignments were confirmed in 3D TOCSY-HMQC and NOESY-HMQC spectra of the complex recorded at 40°C. 44 cross-peaks could be assigned unambiguously in this manner. A further 49 assignments were made by establishing sequential d_{NN} and $d_{\alpha N}$ type NOESY correlations between the amide protons and Cα-protons of adjacent residues [20].

The remaining cross-peaks were assigned on the basis of their ^{15}N chemical shift [21] and the patterns of NOE correlations in a 3D NOESY-HMQC spectrum. The only residues that could not be assigned are Ser-67, Gly-68, Arg-83 and Ser-85 as no cross-peaks with unambiguous correlations could be found for these residues. Only one cross peak in the ^{1}H–^{15}N HSQC spectrum of the complex could not be assigned. The ^{1}H and ^{15}N chemical shift assignments of barnase in the complex with barstar are given in Table I.

Changes in the chemical shifts of both ^{1}H and ^{15}N relative to the free enzyme are observed for nearly all residues in the complex (Table I). However, the effects of binding barstar are reflected more dramatically by changes in the ^{1}H chemical shifts. Changes of $\Delta\delta \geq 0.2$ ppm (chosen arbitrarily) are observed for the backbone amide protons of Ser-28, Val-36, Ser-38, Asn-41, Leu-42, Ile-51, Asp-54, Ser-57, Asn-58, Asn-77, Asp-86, Ile-88 and His-102 (Fig. 2) and for the side-chain H$^\epsilon$ of Arg-83

3.3. Hydrogen deuterium exchange

Hydrogen–deuterium exchange rates were measured by recording a series of ^{1}H–^{15}N HSQC spectra, initially at 20 min intervals, of samples that had been freshly exchanged into D_2O buffer. Differential exchange rates could be determined for a total of 51 backbone amide protons. Of these, it was found that Lys-27, Glu-29, Lys-39, Asn-41, Ser-57, Asn-58, Lys-62, Asn-84, His-

$\rightarrow$

Fig. 1. A region of the ^{1}H–^{15}N HSQC spectra of: (A) free ^{15}N-labelled barnase; and (B) the same sample in the complex formed with unlabelled barstar at 30°C. For clarity, the amide protons from the side chains of glutamine and asparagine residues are not labelled.
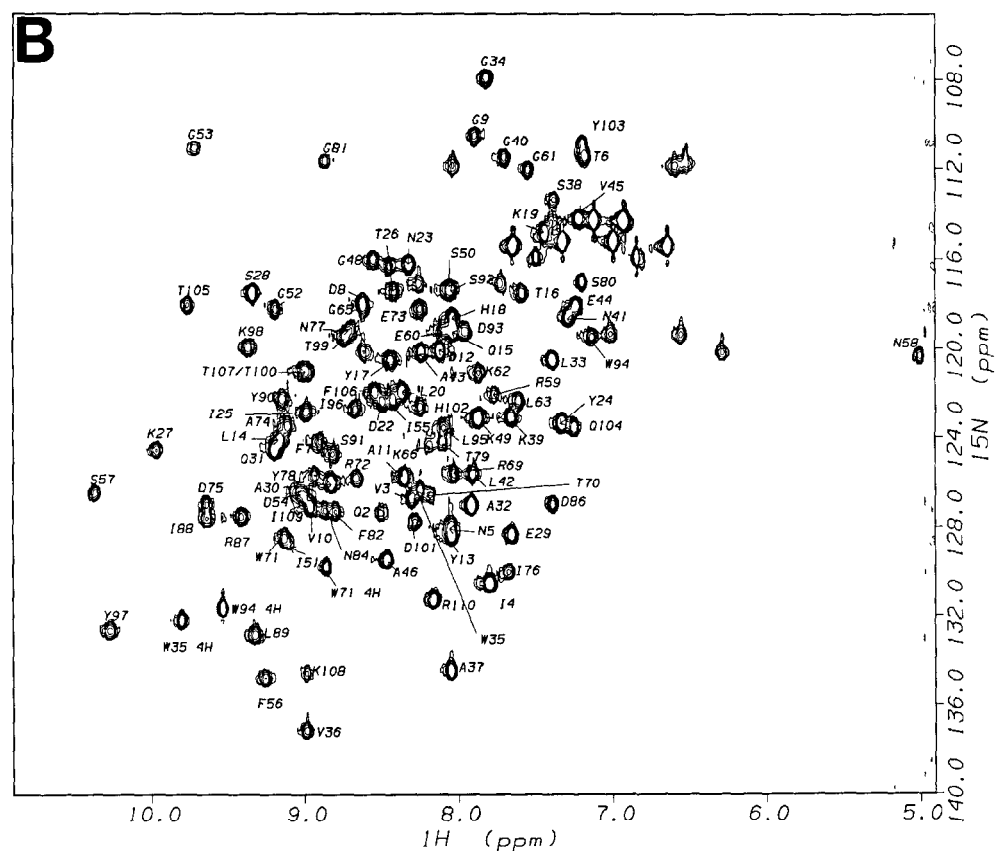
Table I

Amide ¹H and ¹⁵N chemical shift assignments (given in ppm) of barnase in the free enzyme and in the complex with barstar

Residue	Free barnase		Complex		Δδ (complex-free)	
	¹H	¹⁵N	¹H	¹⁵N	¹H	¹⁵N
Q2	8.67	124.55	8.53	127.43	−0.14	2.88
Q2 HD	7.54	116.21				
Q2 HD′	6.88	116.19				
V3	8.31	127.25	8.33	126.76	0.02	−0.49
I4	7.77	130.87	7.84	130.81	0.07	−0.06
N5	8.07	127.77	8.06	128.17	−0 01	0.40
N5 HG	6.64	111.81	6.58	111.77	−0.06	−0.04
N5 HG′	6.48	111.81	6.53	111.77	0.05	−0.04
T6	7 19	111.65	7.17	111.36	−0.02	−0 29
F7	8.97	124.39	8.94	124.32	−0.03	−0 07
D8	8.69	118 10	8.68	117 98	−0.01	−0.12
G9	7.93	110.49	7.90	110.40	−0.03	−0.09
V10	8.94	127.04	9.06	126.68	0.12	−0.36
A11	8.34	125.89	8.37	125.82	0.03	−0.07
D12	8.16	120 00	8.15	120.01	−0.01	0.01
Y13	8.06	128.51	8.05	128.53	−0.01	0.02
L14	9 15	123.97	9.18	124.18	0 03	0.21
Q15	8.06	119.29	8.06	119.33	0.00	0.04
Q15 HD	7.02	115.60				
Q15 HD′	7.44	115.59				
T16	7.62	117.53	7.61	117.57	−0.01	0.04
Y17	8.46	120 48	8.47	120.54	0.01	0.06
H18	8.10	118.54	8.06	118.76	−0.04	0.22
K19	7 45	114.73	7.45	114.73	0.00	0.00
L20	8.38	121.62	8.44	121.91	0.06	0.29
P21						
D22	8.55	122.21	8.57	122.56	0.02	0.35
N23	8 42	116.06	8.34	116.10	−0.08	0.04
N23 HG	6.44	119.11	6.57	119.59	0.13	0.48
N23 HG′	7.08	119.12	7.05	119 59	−0 03	0.47
Y24	7.32	123.09	7 32	123.26	0 00	0.17
I25	9 03	122.20	9.00	122.85	−0.03	0.65
T26	8.53	116.95	8.45	117.43	−0.08	0.48
K27	10.12	125.27	9 97	124.59	−0 15	−0.68
S28	9.13	117.80	9.39	117.58	**0.26**	−0.22
E290	7.70	128.37	7.68	128.39	−0.02	0.02
A30	8 75	126.04	8.85	126.21	0.10	0.17
Q31	9.31	124.12	9.24	124.73	−0.07	0.61
Q31 HD	7.30	114.44				
Q31 HD′	6.89	114.44				
A32	7.95	127.49	7.94	127.05	−0.01	−0.44
L33	7.40	120.73	7.38	120.54	−0.02	**−0.19**
G34	7.78	107.71	7.84	107.96	0.06	0.25
W35	8.31	127.25	8.33	126.76	0.02	−0.49
W35 HE1	9.99	133.07	9.80	132.30	−0.19	−0.77
V36	8.72	137.02	9.01	137.31	**0.29**	0.29
A37	7.92	134.52	8.10	134.48	0.18	−0.04
S38	8.21	114.13	7.41	113.37	**−0.80**	−0.76
K39	7.80	123.10	7.67	123.13	−0.13	0 03
G40	7.66	112.09	7.72	111 48	0.06	−0.61
N41	7.51	118.12	7.29	118.52	**−0.22**	0.40
N41 HG	6.68	112.83	6.62	111 84	−0.06	−0.99
N41 HG′	8.04	112.83	8.07	111.84	0.03	−0.99
L42	8.33	126.74	8.01	125.81	**−0.32**	−0.93
A43	8.11	120.60	8.26	120.02	0.15	−0.58
E44	7.29	118.41	7.24	118.12	−0.05	−0.29
V45	7.26	114.13	7.22	114 07	−0.04	−0.06
A46	8.45	129.40	8.48	129.62	0.03	0 22
P47						
G48	8.60	115.92	8.59	116.08	−0.01	0.16

Table I (continued).

Residue	Free barnase		Complex		$\Delta\delta$ (complex-free)	
	^{1}H	^{15}N	^{1}H	^{15}N	^{1}H	^{15}N
K49	7.86	123.54	7.89	123.24	0.03	−0.30
S50	8.05	117.30	8.06	117.40	0.01	0.10
I51	8.49	127.78	9.16	128.93	**0.67**	1.15
G52	9.21	117.80	9.20	118.25	−0.01	0.45
G53	9.75	111.08	9.75	111.07	0 00	−0.01
D54	8.56	125.44	9.07	126.42	**0.51**	0.98
I55	8.29	122.51	8.47	122.38	0.18	−0.13
F56	9.14	135.39	9.29	134.88	0.15	−0.51
S57	8.59	127.32	10.38	126.50	**1.79**	−0.82
N58	6.35	121.46	5.00	120.34	**−1.35**	−1.12
N58 HD	7.06	115.77				
N58 HD′	7.69	115.76				
R59	7.83	123.66	7.79	122.03	−0.04	−1.63
E60	8.16	119.00	8.11	119.26	−0.05	0.26
G61	7.59	111.07	7.57	112.04	−0.02	0.97
K62	7.91	121.35	7.89	121.09	−0.02	−0.26
L63	7.51	122.48	7.63	122.43	0.12	−0.05
P64						
G65	8.71	118.69	8.65	118.27	−0.06	−0.42
K66	8.21	124.71	8.22	124.51	0.01	−0.20
S67	8.73	124.71				
G68	8.79	119.71				
R69	8.07	125.59	8.06	125.69	−0.01	0.10
R69 HE	8.46	88.41	8.43	88.63	−0.03	**0.22**
T70	8.19	126.33	8.22	126.49	0.03	0.16
W71	9.16	128.37	9.15	128.11	−0.01	−0.26
W71 HE1	8.85	129.67	8.86	129.87	0.01	0.20
R72	8.62	125.72	8.66	125.94	0.04	0.22
E73	8.14	118.10	8.25	118.12	0.11	0.02
A74	9.15	123.97	9.13	123.39	−0.02	−0.58
D75	9.64	127.65	9.67	127.09	0.03	−0.56
I76	7.87	130.72	7.69	130.16	−0.18	−0.56
N77	8.96	119.72	8.71	119.06	**−0.25**	−0.66
N77 HD	6.36	119.85	6.31	120.40	−0.05	0.55
N77 HD′	8.49	119.85	8.65	120.41	0.16	0.56
Y78	8.99	125.87	8.97	125.81	−0.02	−0.06
T79	8.03	123.83	8.17	124.35	0.14	0.52
S80	7.23	117.24	7.21	117.17	−0.02	−0.07
G81	8.79	112.22	8.90	111.61	0.11	−0.61
F82	8.87	126.33	8.91	127.31	0.04	0.98
R83	8.39	123.51				
R83 HE	9.62	88.38	9.99	88.51	**0.37**	0.13
N84	8.99	125.87	8.99	127.18	0.00	1.31
N84 HD	8.35	117.81	8.29	117.11	−0.06	−0.70
N84 HD′	7.89	117.81	7.77	117.11	−0.12	−0.70
S85	8.31	116.91				
D86	7.69	126.45	7.39	127.03	**−0.30**	0.58
R87	9.50	128.06	9.43	127.58	−0.07	−0.48
I88	9.45	127.34	9.66	127.70	**0.21**	0.36
L89	9.43	135.10	9.34	132.86	−0.09	−2.24
Y90	9.34	122.65	9.15	122.18	−0.19	−0.47
S91	8.83	125.14	8.84	124.88	0.01	−0.26
S92	8.05	117.74	8.10	117.59	0.05	−0.15
D93	8.00	119.13	7.96	119.19	−0.04	0.06
W94	7.17	119.55	7.14	119.59	−0.03	0.04
W94 HE1	9.62	131.88	9.56	131.83	−0.06	−0.05
L95	8.14	123.54	8.12	123.65	−0.02	0.11
I96	8.80	122.65	8.69	122.70	−0.11	0.05
Y97	10.35	133.50	10.29	132.72	−0.06	−0.78
K98	9.56	120.58	9.38	119.87	−0.18	−0.71
T99	8.79	119.71	8.75	119.38	−0.04	−0.33
T100	9.06	121.05	9.01	120.96	−0.05	−0.09

Table I *(continued)*.

Residue	Free barnase		Complex		$\Delta\delta$ (complex-free)	
	^{1}H	^{15}N	^{1}H	^{15}N	^{1}H	^{15}N
D101	8.41	126.91	8.29	127.84	−0.12	0.93
H102	8.90	121.32	8.25	122 58	**−0.65**	1.26
Y103	7.31	111.20	7.20	110.87	−0.11	−0.33
Q104	7.27	123.51	7.25	123.53	−0.02	0.02
Q104 HG	6.93	116.35				
Q104 HG'	7.54	116.35				
T105	9.82	118.70	9.77	117.99	−0.05	−0.71
F106	8.66	122.06	8.59	122.09	−0.07	0.03
Y107	9 09	120.15	9.01	120.96	−0.08	0.81
K108	8.94	134.10	9 04	134.62	0.10	0.52
I109	8 99	125.87	9.10	126.45	0.11	0.58
R110	8.17	131 15	8.19	131.49	0.02	0.34

Amide protons which show changes of >0.2 ppm are highlighted in bold type

102, Tyr-103, Gln-104 and Thr-105 are strongly protected from exchange with solvent; Gly-61, Phe-82, Arg-87 and Asp-101 are mildly protected from exchange; and Val-36 and Val-45 are weakly protected from exchange. The only amide proton which shows an enhanced exchange rate is that of Ala-32. With the exception of Arg-87 it is not possible to determine the changes in protection factors for any of these amide protons because they are all exchanging far too rapidly in the free protein and all signal from these protons decays within the dead time of the experiment.

4. DISCUSSION

In the barnase–barstar complex those barnase residues that show changes in amide–proton chemical shifts of >|0.2| ppm or significant differences in exchange with solvent relative to the free enzyme are located on the opposite side of the β-sheet to α-helix$_1$ (residues 6–18). Exchange rates can be measured for several residues in this helix and none of these residues show any significant differences. This indicates that the binding of barstar does not involve interaction with this side of the molecule. Changes are observed for residues in the guanosine-binding loop (Ser-57, Asn-58, Gly-61 and Lys-62); the active-site loop (Asp-101, His-102, Tyr-103, Gln-104 and Thr-105) which packs against the guanosine binding loop; the N-terminus of α-helix$_2$ (Lys-27. Ser-28 and Glu-29); β-strand$_1$ (Ile-51 and Asp- 54), which packs against α-helix$_2$; and β-strand$_3$ (Asp- 86, Arg-87 and Ile-88) which lies at the bottom of the broad groove and forms part of the active site. These residues are all located in regions of the molecule that are involved in catalysis or substrate binding. Significant changes are observed in other regions of the molecule and are, generally, located at the opposite end of the
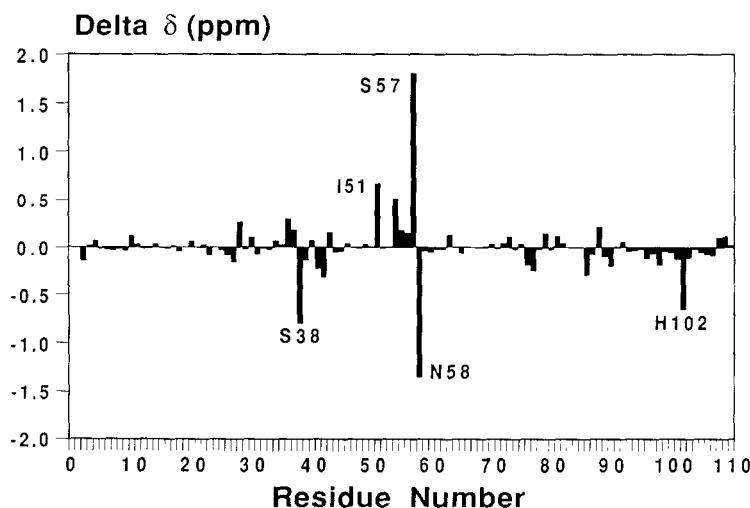

Fig. 2. Changes in the backbone amide- proton chemical shifts of barnase on binding barstar. The value of (Delta δ) is calculated as δ(complexed)-δ(free).

molecule to the active-site loop: the C-terminus of α-helix$_2$ (Ala-32); loop$_2$ (Val-36, Ser-38 and Lys-39); α-helix$_3$ (Asn-41, Leu-42 and Val-45); and loop$_4$ (Phe- 82, Arg-83 and Asn-84) which, in conjunction with α-helix$_3$, forms one edge of the broad groove. These results are summarised in Fig. 3 and Fig. 4.

The largest changes are observed for residues which are located in either the guanosine-binding loop, residues 56–63, or the active-site loop, residues 101–105, which packs against it. In particular Ser-57 is shifted down-field by 1.79 ppm in the ^{1}H dimension in contrast, Asn-58 shifts up-field by 1.35 ppm (to 5.00 ppm). Generally changes of these magnitudes are explained by the existence of aromatic ring-current contributions to the magnetic environment of the nucleus. However, the down-field shift of the amide proton of Ser-57 is much greater than that that can be induced even by van der Waals' contact of the amide proton with a tryptophan ring [22,23]. It has been observed that the amide proton of Ser-57 is involved in forming a hydrogen bond to the guanosine base when barnase binds to 3'-GMP (E. Meiering and ARF, unpublished data). If Ser-57 forms a new hydrogen bond when barstar binds, this would induce an additional down-field shift which may explain the observed large down-field shift. The upfield shift to 5.00 ppm observed for Asn-58 may be explained by an interaction with an aromatic residue. Up-field shifts of >2 ppm can be induced by the close approach of a
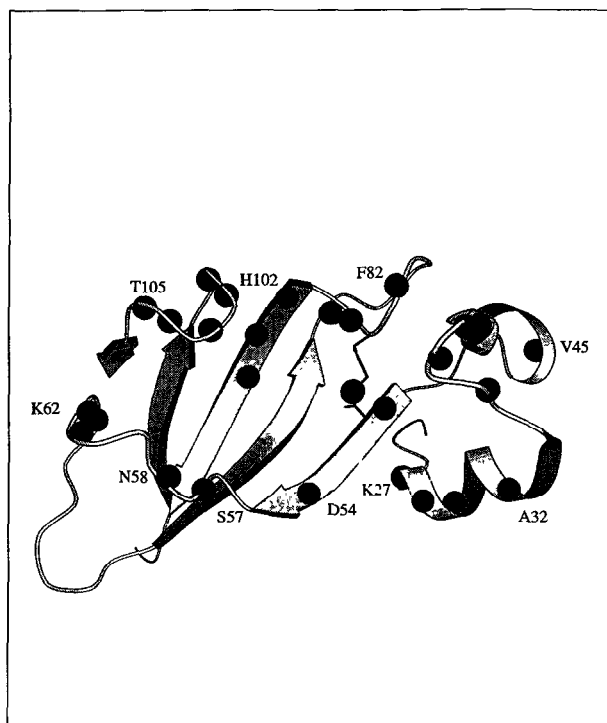

Fig. 4. View of the NMR solution structure of barnase from above the β-sheet showing those amide protons affected by the binding of barstar. The α-helix formed by residues 6–18 lies below the plane of the page and is not shown.

proton to a tryptophan ring. Similar changes in chemical shift to those observed here are observed for residues 57 and 58 when barnase binds 3'-GMP (Meiering and Fersht, unpublished data) however the magnitude of the shift of Asn-58 is smaller in this latter case. There are three tryptophan residues in barstar, and it is possible that one of these mimics the binding of the guanosine base of the normal substrate.

Loop$_5$, which contains the active site histidine, His-102, packs against the guanosine binding loop. All the residues within this loop are strongly protected from exchange when barstar binds and in addition the amide proton of His-102 exhibits a large up-field shift of 0.65 ppm. These observations are consistent with the suggestion that an aromatic residue from barstar may be involved in binding in this region.

The changes observed for other residues most probably result from direct interaction with barstar. It is possible, however, that some of the changes arise from intermolecular perturbations that are transmitted allosterically from the binding site to other regions of the molecule and it is not possible to rule out such effects. However, we do not observe any significant changes for the amide protons of residues located in α-helix$_1$ which is located on the opposite face to the proposed binding site.

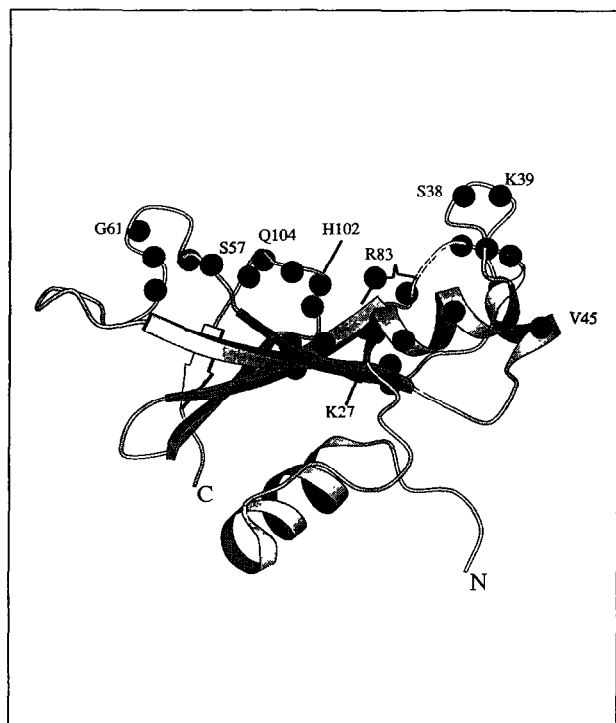In only one case, Ala-32, do we observe an increase

Fig. 3. View of the NMR solution structure of free barnase showing those amide protons which exhibit significant changes in either chemical shift or hydrogen exchnage rates on binding barstar. The diagram was produced using the program MOLSCRIPT [24].

in the rate of hydrogen–deuterium exchange. This suggests that the hydrogen bond formed between the NH of Ala-32 and the carbonyl of Ser-28 in free barnase is disrupted by the binding of barstar. Other residues within this region show enhanced protection from exchange and this suggests that any disruption of the secondary structure is localised to a few residues.

From these studies, we conclude that barstar binds to barnase in a manner that sterically blocks the active site. The main interactions appear to involve recognition of the major substrate binding site, the 'guanosine-binding loop' formed by residues 56–63, and the active site loop, residues 99–105, which are located at one end of the molecule. It is clear, however, that other sites in the enzyme are also important in the binding of the inhibitor. These include Lys-27 at the N-terminus of α-helix$_2$ that has been identified as an important contributor to the activity of the enzyme [14] and also the first strand of the β-sheet against which α-helix$_2$ packs. There is evidence that the binding site extends along almost the whole length of the molecule. This relatively large binding site allows the formation of many new interactions between the enzyme and its inhibitor and may explain efficiency of the inhibitor and the stability of the enzyme–inhibitor complex. The general topology of the barstar binding site has been confirmed by mutation of residues within the proposed binding site to asses the contributions that they make to the stability of the complex [11].

REFERENCES

[1] Janin, J. and Chothia, C. (1990) J. Biol. Chem. 265, 16027–16030.

[2] Hill, C., Dodson, G., Heinmann, U., Saenger, W., Mitsui, Y., Nakamura, K., Borisov, S., Tischenko, G., Polyakov, K. and Pavlovsky, S. (1983) Trends Biochem. Sci 8, 364–369.

[3] Sevcik, J., Sanishvili, R.G., Pavlovsky, A.G. and Polyakov, K.M. (1990) Trends Biochem. Sci. 15, 158–162.

[4] Mauguen, Y., Hartley, R.W., Dodson, E J., Dodson, G.G., Bicogne, G., Chothia, C. and Jack, A. (1982) Nature 297, 162–164.

[5] Baudet, S. and Janin, J. (1991) J. Mol. Biol. 214, 123–132

[6] Bycroft, M, Sheppard, R.N., Lau, F.T.-K. and Fersht, A.R. (1990) Biochemistry 29, 7245–7432.

[7] Bycroft, M., Ludvigsen, S., Fersht, A.R. and Poulsen, F.M. (1991) Biochemistry 30, 8697–8701

[8] Smeaton, J.R. and Elliot, W.H (1967) Biochim. Biophys. Acta 145, 547–560.

[9] Hartley, R.W. (1989) Trends Biochem. Sci. 14, 450–454.

[10] Hartley, R.W. and Smeaton, J.R. (1973) J. Biol. Chem. 248, 5624–5626.

[11] Schreiber, G and Fersht, A R. (1993) Biochemistry 32, 4322–4329.

[12] Day, A.G., Parsonage, D., Ebel, S., Brown, T. and Fersht, A.R. (1992) Biochemistry 31, 6390–6395.

[13] Paddon, C.J. and Hartley, R.W. (1987) Gene 53, 11–19.

[14] Mossakowska, D.E., Nyberg, K. and Fersht, A R. (1989) Biochemistry 28, 3843–3850.

[15] Studier, F.W (1991) J. Mol. Biol 219, 37–44.

[16] Levy, G. and Lichter, R L. (1979) Nitrogen-15 Nuclear Magnetic Resonance Spectroscopy, John Wiley & Sons, New York.

[17] Bax, A., Ikura, M., Kay, L.E., Torchia, D.A. and Tschudin, R. (1990) J. Magn. Reson. 86, 304–318.

[18] Gronenborn, A.M., Bax, A., Wingfield, P.T. and Clore, G.M (1989) FEBS Lett. 243, 93–98.

[19] Marion, D., Driscoll, P.C., Kay, L.E., Wingfield, P.T, Bax, A., Gronenborn, A M. and Clore, G.M. (1989) Biochemistry 28, 6150–6156.

[20] Wüthrich, K. (1986) NMR of Proteins and Nucleic Acids. John Wiley & Sons, New York

[21] Neri, D., Wider, G. and Wuthrich, K. (1992) Proc. Natl. Acad Sci. USA 89, 4397–4401.

[22] Giessner-Prettre, C and Pullman, B. (1971) J. Theor. Biol. 31, 287–294.

[23] Giessner-Prettre, C. and Pullman, B. (1981) Biochem. Biophys. Res. Commun. 101, 921–926

[24] Kraulis, P.J. (1991) J. Appl. Crystall. 24, 946–950.